European Journal of Cardio-Thoracic Surgery 45 (2014) 1089–1096
doi:10.1093/ejcts/ezt660 Advance Access publication 20 February 2014

ORIGINAL ARTICLE

Mechanisms of functional mitral regurgitation in cardiomyopathy secondary to anterior infarction

Marek A. Deja[a,*], Piotr Janusiewicz[a], Katarzyna Gruszczyńska[b], Jolanta Biernat[c], Jan Baron[b], Marcin Malinowski[a], Krzysztof S. Gołba[c] and Stanisław Woś[a]

[a] 2nd Department of Cardiac Surgery, Medical University of Silesia, Katowice, Poland
[b] Department of Radiology and Nuclear Medicine, Medical University of Silesia, Katowice, Poland
[c] Department of Cardiology, Medical University of Silesia, Katowice, Poland

* Corresponding author. 2nd Department of Cardiac Surgery, Medical University of Silesia, Ziołowa 47, 40-635 Katowice, Poland. Tel/fax: +48-32-2526093; e-mail: mdeja@sum.edu.pl (M.A. Deja).

Received 12 May 2013; received in revised form 9 October 2013; accepted 16 October 2013

Abstract

OBJECTIVES: It remains unclear why some patients with cardiomyopathy secondary to anterior infarction do, and others do not develop functional mitral regurgitation (MR).

METHODS: Thirty-six patients after anterior infarction with ejection fraction (EF) below 35%, 18 with no/trivial and 18 with moderate/severe MR, underwent cardiac magnetic resonance imaging. Parameters describing the geometry of the mitral valve, subvalvular apparatus and left ventricle were measured.

RESULTS: The septolateral and commissure-to-commissure mitral annular diameters were bigger in patients with MR. The odds ratio (OR) of developing regurgitation was 25.0 (95% confidence interval [95% CI] 4.3–144.3; $P < 0.001$) for end-systolic septolateral mitral annulus diameter above 20 mm/m^2. MR was less likely in patients with straighter posterior papillary muscle (OR 0.040, 95% CI 0.007–0.23; $P < 0.001$—for the angle between muscle axis and mitral annulus plane >81°), and more likely (OR 7.9, 95% CI 1.6–39.4; $P = 0.008$) with posterior papillary muscle tethering >23 mm/m^2. Regurgitation was less likely (OR 0.032, 95% CI 0.003–0.33; $P = 0.001$) with anterolateral papillary muscle tip to ipsilateral mitral annulus distance in end-diastole longer than 13 mm/m^2. Left ventricular EF, volumes and the overall end-systolic and end-diastolic wall thicknesses did not differ between the groups. Patients with MR had thinner myocardium proximal to the base of the anterior and distal to the base of the posterior papillary muscle.

CONCLUSIONS: Inferior extension of anterior infarction and more leaning posterior papillary muscle are the major components resulting in the development of ischaemic MR in patients with cardiomyopathy secondary to anterior infarction. Shorter chordae tendineae may constitute the anatomical background that makes the development of ischaemic MR more likely.

Keywords: Mitral regurgitation • Pathophysiology (mitral valve) • Cardiomyopathy • Magnetic resonance imaging

ADULT CARDIAC

INTRODUCTION

Chronic ischaemic mitral regurgitation (MR) is associated with increased mortality and incidence of heart failure [1–3]. Many experimental animal studies showed that apical and posterior displacement of papillary muscles (primarily posteromedial) and subsequent leaflet tethering play a major role in the development of ischaemic functional MR [4–7]. Besides, progressive dilatation of the mitral annulus secondary to left ventricular (LV) enlargement leads to decreased leaflet coaptation in systole [4, 6, 8–11]. Echocardiographic and cardiac magnetic resonance (CMR) studies confirmed the role of these mechanisms in the aetiology of ischaemic MR in patients [12–14]. Ischaemic MR is more common after an inferior myocardial infarction [6, 12, 13, 15, 16]. Geometric changes of the subvalvular apparatus lead to the development of MR after an inferobasal myocardial infarction even in ventricles with relatively well-preserved global function [5, 6, 12]. Meanwhile, ischaemic MR after anteroapical infarction requires more advanced LV remodelling to appear [13]. It remains unclear why some patients with ischaemic cardiomyopathy secondary to anterior infarction develop functional MR, while others with a seemingly similar degree of LV remodelling present with a competent mitral valve.

MATERIALS AND METHODS

Sixty-five patients with stable coronary artery disease and LV ejection fraction (EF) below 35% underwent CMR imaging in preparation for coronary bypass surgery in our institution. All patients had suffered anterior myocardial infarction in the past and were studied to assess whether they were candidates for surgical ventricular restoration. Of them, we selected a group of 18 patients with most severe and 18 with most trivial MR based on echocardiography to look for the geometric correlates of ischaemic MR in this type of remodelled left ventricle.

© The Author 2014. Published by Oxford University Press on behalf of the European Association for Cardio-Thoracic Surgery. All rights reserved.

CMR studies were performed using a 1.0-T Unit (Magnetom Harmony, Siemens) with magnetic gradient amplitude 40 mT, slew rate 200 mT/m/s and a dedicated four-element phase-array receiver coil. An examination protocol consisted of an spin echo/T_1-weighted sequence, 'dark blood' images in the axial plane and a TruFISP cine ECG-gated sequence. The imaging parameters were: 19 temporal phases per slice, 24 segments, voxel size 2.1 × 2.1 × 8 mm, repetition time 3.0–3.6 ms, time-to-echo 1.2–1.4 ms, flip angle 67° and number of averages 1. The two-chamber view consisted of 3.8 mm slices (with zero gap) with the central slice passing through the LV apex and LV base (parallel to the septum). The four-chamber view consisted of 3.8 mm slices with the central slice plane passing through the apex and bisecting the mitral valve at the base. Using the end-diastolic four-chamber view, short-axis slices of 8 mm, with no interslice gap, perpendicular to the interventricular septum and extending beyond the valve

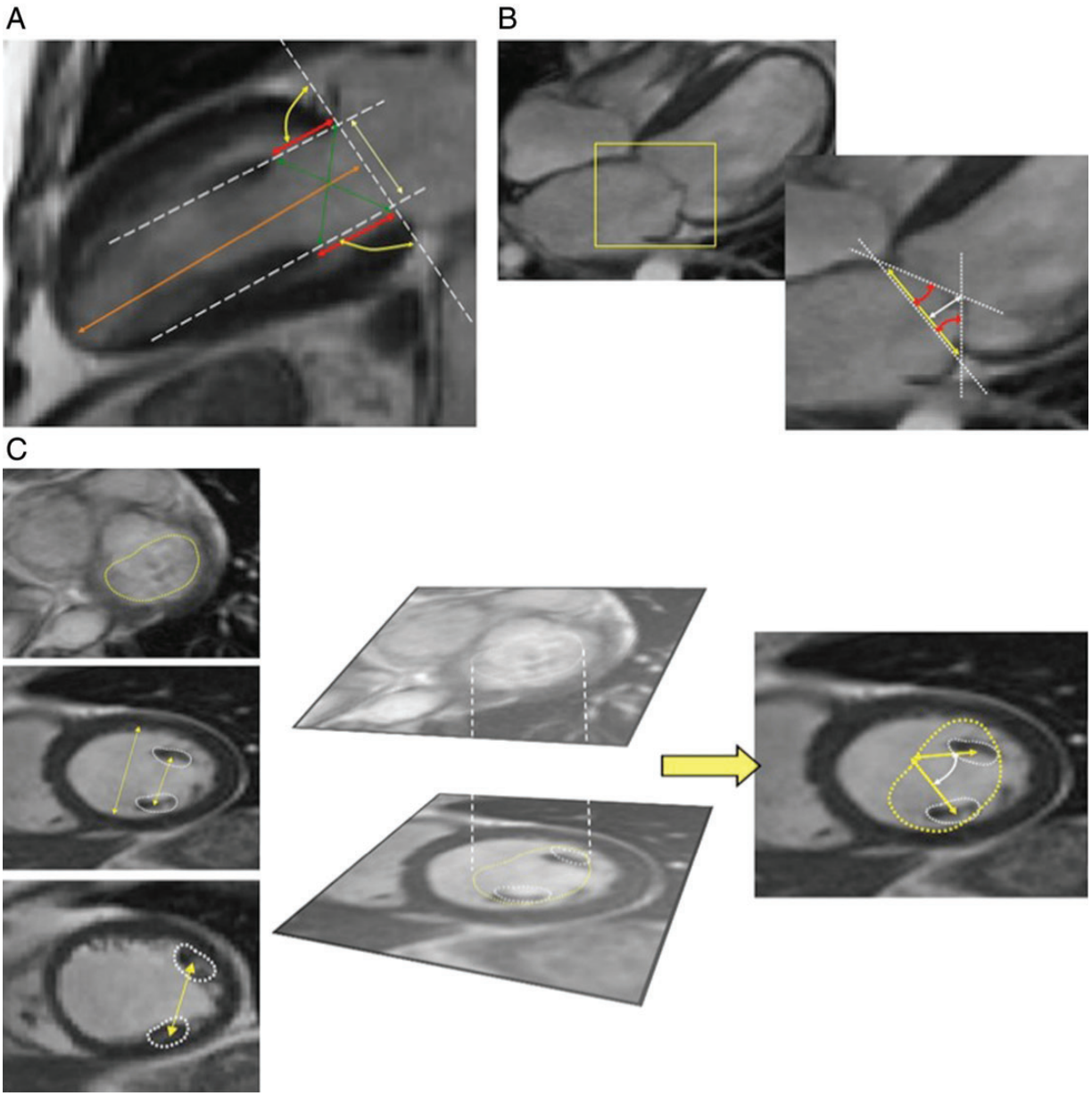

Figure 1: The parameters measured on CMR imaging. (**A**) The two-chamber views were used to measure: the angles between the mitral annulus plane and the long axis of the PPM and APM, respectively (yellow arrows), the distances from the PPM tip to the ipsilateral (red arrow) and contralateral (green arrow) aspects of the mitral annulus, as well as the distances from the APM tip to these aspects of the mitral annulus, the length of the LV (from the mitral annulus plane to the apex—orange arrow) and the commissure-to-commissure mitral annulus diameter. All measurements were performed in both end-systole and end-diastole. (**B**) From the four-chamber views, the septolateral mitral annulus diameter was measured (yellow arrow), in both end-systole and end-diastole. We also measured the angles of the anterior and posterior mitral leaflets to the mitral valve plane (red arrows), as well as the tenting height (coaptation depth—distance from the annulus plane to the leaflet coaptation point) and tenting area (area between leaflets of mitral valve and mitral annulus) in end-systole. (**C**) The short-axis views were used to measure the mitral annulus area, the distance between the tips and bases of papillary muscles and the LV diameter at the level of the papillary muscle tips in both end-systole and end-diastole. In addition, we superimposed the slice containing papillary muscle tips on the mitral annulus plane (on the right). We next constructed two lines from the saddle horn to both the papillary muscle tip projections, and measured the length of each line and the angle between them.

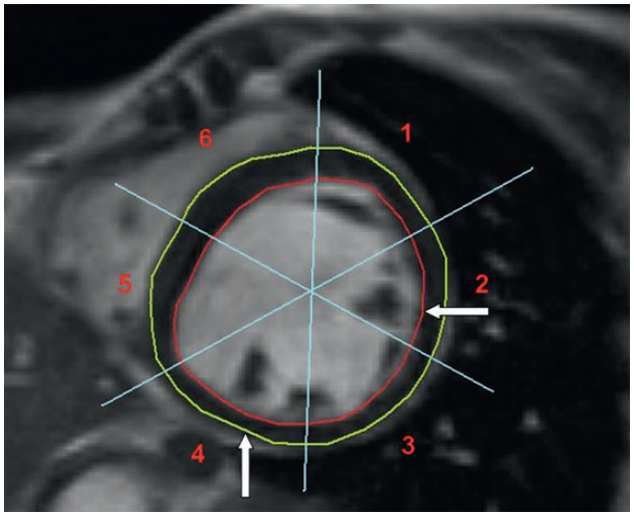

Figure 2: Segments of Layer 7 of the LV wall containing attachments of papillary muscles (details in the text).

plane were planned. The most apical slice was set beyond the myocardium.

Figures 1 and 2 summarize the measurements performed on CMR images.

All measurements were performed by a single investigator (Piotr Janusiewicz) who was unaware of the patients' mitral valve function on echocardiography. Each measurement was performed at least twice, and the median was then used for further analysis. The coefficient of variation for measurements of distance varied from 2.2 to 5.5%, and equalled 6.3–7.1% for measurements of angle and 4.5–6.7% for measurements of area. All parameters (apart from angles) were normalized to the patient's body surface area.

LV end-diastolic and end-systolic volume indexes as well as the EF were assessed by means of a dedicated workstation (Leonardo, Siemens), using the CMR imaging software (Argus, Siemens). Endocardial and epicardial contours were manually drawn on short-axis images by a single operator (Katarzyna Gruszczyńska) who was unaware of the echocardiography results. Papillary muscles and endocardial trabeculations were excluded (Fig. 2). A 'slice-omission' technique was used to correct for the through-plane motion: basal slices with an incomplete muscular ring of less than 75% were omitted as 'atrial'.

The LV wall was divided into six segments at each short-axis view layer, with the first segment starting at the interventricular septum–anterior wall junction (Fig. 2). We measured end-systolic and end-diastolic LV wall thickness in every segment. Up to 14 layers per LV were obtainable. As we were particularly interested in the LV wall thickness in relation to papillary muscle attachment, the LV layer containing papillary muscle bases was numbered as 7 and all the other 8-mm layers were numbered accordingly, starting from the lowest number at the base to the highest at the apex. The anterolateral papillary muscle (APM) was therefore always attached to Segment 2 of Layer 7, and the posteromedial papillary muscle (PPM) to Segment 4 of the same layer (Fig. 2). We also used the median thickness of all segments as an overall estimate of the LV wall thickness in the given patient. As Layers 1 and 14 were measurable in less than half of the patients, these layers were omitted when comparing the overall LV wall thickness between the groups.

The patients' characteristics (categorical data) are presented as percentages and compared using Fisher's exact test. The quantitative data are presented as the median with first and third quartiles. Normally distributed data were compared using an independent data *t*-test. The Mann–Whitney *U*-test was used otherwise.

To further assess the association of CMR-measured parameters with the presence of MR, the parameters with $P<0.1$ were dichotomized, using as the cut-off the value with the highest sensitivity and specificity to predict MR on receiver operator characteristic curve analysis. Next, the occurrence of MR in patients with the parameters above and below the cut-off value was compared using a χ^2 test, and the odds ratio (OR) for MR was calculated.

RESULTS

The patients

The patients were divided into two groups—with no or trivial MR and with moderate-to-severe MR. The echocardiographic assessment of mitral valve function is summarized in Table 1.

The groups of patients were otherwise quite similar (Table 2).

Mitral valve

When analysing the parameters describing the valve itself, we found that not only septolateral but also commissure-to-

Table 1: Echocardiographic characteristics of mitral valve function in both study groups

	No or trace MR (n = 18)	Moderate–severe MR (n = 18)	P-values
MR grade	None 8 (44%), trace 10 (56%)	Moderate 9 (50%), severe 9 (50%)	
PISA diameter [mm]	0 (0–3)	7 (5–9)	<0.001
VC [mm]	0 (0–0)	6 (3–7)	0.002
LA area [cm^2]	21.6 (17.9–23.8)	22.0 (21.1–24.5)	0.02
Regurgitation jet area [cm^2]	2.3 (0–3.6)	14.0 (9.0–17.0)	<0.001
Jet area/LA area	0.11 (0.0–0.15)	0.66 (0.39–0.72)	<0.001

The data are presented as the median with first and third quartiles.
MR grade: mitral regurgitation grade as assessed by the echocardiographist; PISA: proximal isovelocity surface area; VC: vena contracta; LA: left atrium.

Table 2: Patient characteristics

	No or trace MR (n = 18)	Moderate–severe MR (n = 18)	P-value
Age (years)	60.4 (53.1–67.5)	60.0 (54.3–66.9)	0.8
Females	2 (11%)	3 (17%)	1.0
Angina CCS class ≥3	5 (27%)	5 (27%)	1.0
Dyspnoea NYHA class ≥3	3 (17%)	3 (17%)	1.0
NYHA class ≥3 within last 3 months	14 (78%)	13 (72%)	1.0
Anterior MI in the past	18 (100%)	18 (100%)	1.0
PCI in the past	3 (17%)	6 (33%)	0.4
LM disease	3 (17%)	4 (22%)	1.0
Triple vessel disease	12 (67%)	10 (56%)	0.7

CCS: Canadian Cardiovascular Society; LM: left main coronary artery; MI: myocardial infarction; MR: mitral regurgitation; NYHA: New York Heart Association; PCI: percutaneous coronary intervention.

Table 3: Geometric parameters of the mitral valve in patients with ischaemic cardiomyopathy with and without significant mitral regurgitation as measured in end-systole and end-diastole (n = 18 in each group)

	MR	End-systole		End-diastole	
		Median (Q1–Q3)	P-values	Median (Q1–Q3)	P-values
MV area [cm^2/m^2]	0	4.03 (3.85–4.67)	0.10	4.61 (4.03–5.07)	0.037
	1	4.62 (4.05–5.69)		5.02 (4.55–6.30)	
Tenting height [mm/m^2]	0	3.8 (3.1–4.2)	0.46	–	–
	1	3.9 (2.9–4.7)		–	
Tenting area [cm^2/m^2]	0	1.11 (1.05–1.25)	0.049	–	–
	1	1.31 (1.13–1.55)		–	
S-L diameter of the MV annulus [mm/m^2]	0	18.4 (17.7–20.2)	0.002	20.4 (19.5–22.1)	0.037
	1	21.8 (20.9–22.9)		22.4 (21.7–23.8)	
C-C diameter of the MV annulus [mm/m^2]	0	18.2 (17.6–20.1)	0.037	19.4 (18.3–21.0)	0.023
	1	19.6 (18.4–22.2)		20.8 (19.4–23.6)	
Angle between the AML and the MV annulus plane [°]	0	23.3 (17.9–26.1)	0.024	–	–
	1	18.0 (17.6–21.8)		–	
Angle between the PML and the MV annulus plane [°]	0	40.8 (34.1–51.3)	0.37	–	–
	1	39.3 (36.5–42.8)		–	
S-L/C-C ratio	0	1.03 (0.96–1.11)	0.13	1.08 (0.96–1.13)	0.72
	1	1.07 (1.00–1.17)		1.05 (0.99–1.12)	

All measurements (apart from angles) are indexed to the body surface area.
MV: mitral valve; S-L: septolateral; C-C: commissure-to-commissure; AML: anterior mitral leaflet; PML: posterior mitral leaflet; S-L/C-C ratio: ratio of the septolateral diameter to the intercommissural diameter of the mitral valve annulus; MR: mitral regurgitation; Q1: first quartile; Q3: third quartile.

commissure mitral annulus diameter was bigger in patients with MR in both end-systole and end-diastole (Table 3). The end-diastolic mitral annulus area was also significantly enlarged. The septolateral to intercommissural distance ratio was above 1 in both end-systole and end-diastole in all patients. The tenting area was significantly bigger in patients with MR, while tenting height was similar in both groups.

An end-systolic septolateral annulus diameter was the parameter most strongly associated with the presence of MR in univariate analysis (Supplementary Table 1). The OR of developing MR was 25.0 (95% confidence interval [95% CI] 4.3–144.3; $P < 0.001$) for the end-systolic septolateral mitral annulus diameter of >20 mm/m^2.

Subvalvular apparatus

We observed significantly increased distance (tethering) of the PPM tip from the contralateral mitral annulus in end-systole in patients with MR (Table 4). The muscle was also more leaning with a smaller angle in relation to the mitral annulus plane in end-systole and end-diastole. Meanwhile, the distance of the APM tip to the mitral annulus appeared smaller.

We failed to show the difference of the papillary muscle position in relation to mitral annulus saddle horn between the groups. In patients with MR, the distance between papillary muscle tips and bases tended to be increased in end-diastole.

Table 4: Geometric parameters of the subvalvular apparatus in patients with ischaemic cardiomyopathy with and without significant mitral regurgitation as measured in end-systole and end-diastole (n = 18 in each group)

	MR	End-systole		End-diastole	
		Median (Q1–Q3)	*P*-values	Median (Q1–Q3)	*P*-values
MV saddle horn to the APM tip projection distance [mm/m^2]	0	12.9 (10.9–14.8)	0.083	15.3 (13.2–18.0)	0.49
	1	14.0 (12.2–17.9)		16.2 (13.9–18.7)	
MV saddle horn to the PPM tip projection distance [mm/m^2]	0	14.5 (11.8–18.5)	0.59	15.5 (14.3–18.4)	0.21
	1	15.8 (12.9–18.1)		16.9 (14.8–19.7)	
Angle between lines connecting the MV saddle horn with papillary muscle tip projections [°]	0	75.0 (60.5–85.8)	0.47	72.0 (60.0–86.4)	0.64
	1	69.0 (62.0–79.8)		76.5 (63.8–85.5)	
Distance between papillary muscle tips [mm/m^2]	0	15.7 (15.0–17.2)	0.15	18.4 (16.7–19.4)	0.067
	1	18.5 (15.4–20.8)		21.2 (17.2–24.8)	
Distance between papillary muscle bases [mm/m^2]	0	16.9 (14.9–18.2)	0.42	18.7 (16.2–20.8)	0.055
	1	17.1 (15.1–23.6)		19.3 (17.5–25.2)	
Distance from the PPM tip to the ipsilateral MV annulus [mm/m^2]	0	16.9 (14.9–18.6)	0.32	18.1 (15.5–20.0)	0.10
	1	15.6 (14.0–17.9)		16.5 (15.1–18.3)	
PPM tethering [mm/m^2]	0	22.7 (20.0–23.9)	0.035	25.5 (22.7–27.7)	0.36
	1	24.3 (22.5–26.9)		25.8 (23.8–28.1)	
APM tethering [mm/m^2]	0	22.1 (20.7–24.2)	0.039	23.2 (21.6–25.7)	0.13
	1	20.9 (19.2–22.9)		22.1 (20.0–23.8)	
Distance from the APM tip to the ipsilateral MV annulus [mm/m^2]	0	14.1 (12.6–16.2)	0.068	15.7 (14.1–16.0)	0.003
	1	12.0 (11.2–15.5)		12.4 (11.1–14.9)	
Angle between the long axis of the PPM and the MV plane [°]	0	85.3 (81.5–89.3)	<0.001	79.5 (76.0–87.4)	0.053
	1	74.3 (71.4–80.3)		74.0 (71.5–81.5)	
Angle between the long-axis of the APM and the MV plane [°]	0	73.3 (66.5–88.8)	0.61	74.3 (65.0–82.1)	0.20
	1	76.0 (70.5–80.8)		79.0 (74.5–82.0)	

The first three parameters were measured after superimposing the layer containing papillary muscle tips and the layer containing the MV (see methods). All measurements (apart from angles) are indexed to the body surface area.
MV: mitral valve; PPM: posteromedial papillary muscle; APM: anterolateral papillary muscle; PPM: tethering—distance from the PPM tip to the contralateral mitral annulus; APM: tethering—distance from the APM tip to the contralateral mitral annulus; MR: mitral regurgitation; Q1: first quartile; Q3: third quartile.

Table 5: Parameters of the left ventricle in patients with ischaemic cardiomyopathy with and without significant mitral regurgitation as measured in end-systole and end-diastole

	MR	*N*	End-systole		End-diastole	
			Median (Q1–Q3)	*P*-values	Median (Q1–Q3)	*P*-values
LV diameter [mm/m^2]	0	18	31.2 (27.2–33.0)	0.11	36.7 (30.8–39.2)	0.18
	1	17	31.9 (27.8–38.8)		38.6 (32.1–44.2)	
LV length [mm/m^2]	0	18	52.9 (49.8–56.2)	0.65	53.5 (50.4–58.5)	0.72
	1	18	52.0 (50.4–61.8)		52.5 (50.7–60.7)	
Sphericity index	0	18	0.57 (0.54–0.63)	0.20	0.69 (0.62–0.74)	0.29
	1	17	0.61 (0.55–0.68)		0.70 (0.63–0.76)	
LV volume [ml/m^2]	0	18	112 (99–133)	0.13	147 (131–177)	0.20
	1	17	138 (90–175)		165 (116–224)	
Ejection fraction [%]	0	18		23.3 (20.5–28.0)		0.29
	1	17		21.0 (16.5–26.5)		

All measurements (apart from ejection fraction) are indexed to the body surface area.
LV: left ventricle; Sphericity index: LV diameter/LV length; MR: mitral regurgitation; Q1: first quartile; Q3: third quartile.

In univariate analysis, two parameters describing the geometry of PPM were very strongly associated with the presence of MR (Supplementary Table 2). MR was less likely in patients with straighter PPM (OR 0.04, 95% CI 0.007–0.23; $P < 0.001$— for the angle between PPM axis and mitral annulus plane >81°), and more likely (OR 7.9, 95% CI 1.6–39.4; $P = 0.008$) with PPM tip distance from contralateral annulus (tethering) >23 mm/m^2. The strongest end-diastolic correlate was the APM tip distance from the ipsilateral annulus. MR was less likely (OR 0.03, 95% CI 0.003–0.33; $P = 0.001$) in patients with this distance greater than 13 mm/m^2.

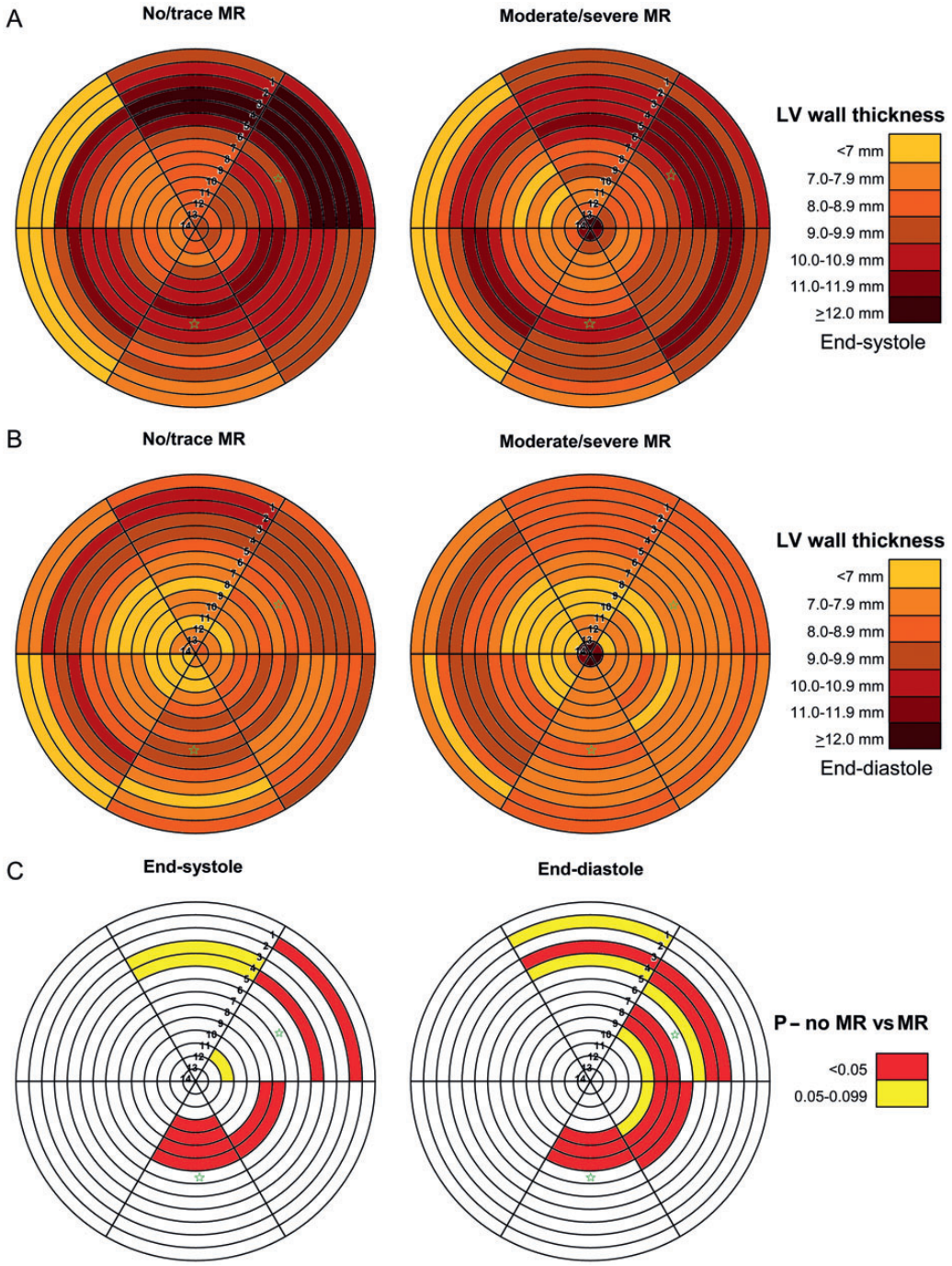

Figure 3: LV wall thickness at each segment. (**A**) The median muscle thickness in end-systole. (**B**) The median muscle thickness in end-diastole. (**C**) Segments thinner in patients with MR in both end-systole and end-diastole are shown together with *P*-values. In all figures, the position of papillary muscle attachment is marked.

Left ventricle

In 1 patient with significant MR, the CMR study had to be interrupted during short-axis image acquisition and, therefore, full LV analysis is available in only 17 patients of the MR group (Table 5).

The EF was 23.3% (20.5–28.0%) in patients with no MR and 21.0% (16.5–26.5%) in patients with moderate-to-severe MR ($P = 0.3$).

The overall end-systolic LV wall thickness (median of all measured segments) was 9.2 (8.9–9.9) mm in patients with no MR and 8.9 (8.3–9.7) mm in the MR group ($P = 0.2$). The end-diastolic thickness was 7.9 (7.4–8.5) mm and 7.6 (7.0–8.4) mm ($P = 0.3$), respectively.

We managed to identify two areas of significantly thinner myocardium in patients with MR: proximal to the base of the APM (Segments 1 and 2 of Layers 4 and 5) and distal to the base

of the PPM (Segments 3 and 4 of Layers 8 and 9, and Segment 4 of Layers 10 and 11). The details for both end-systole and end-diastole are presented in Fig. 3 and also in Supplementary Table 3.

DISCUSSION

Both experimental and clinical studies found inferior myocardial infarction as one of the strongest predictors of the development of ischaemic MR [5, 6, 12, 13]. Authors have studied in detail the geometric changes of LV shape and the subvalvular apparatus leading to appearance of functional MR in spite of relatively well-preserved LV function [5, 12, 13]. Our study is quite different. We studied exclusively patients with a history of anterior or anteroapical myocardial infarction and severely depressed LV function. We always remained puzzled as to why some patients with advanced LV remodelling secondary to anterior infarction develop MR, while others with a similar degree of LV dysfunction remain free of significant MR.

It seems that we managed to ascertain a good group of patients to study this problem. Patients in both groups had a very low EF and increased LV volumes and diameters. The LV sphericity indices remained very similar, indicating a similar degree of overall LV remodelling. Meanwhile, many other studied parameters were found to differ greatly between the groups.

Although the mitral annulus had lost its normal shape and became more circular in all studied patients, as evidenced by the ratio of septolateral to intercommissural diameter greater than 1, not all patients developed MR. In patients with MR, not only the septolateral diameter but also the intercommissural distance of the mitral annulus was significantly greater. This echoes many earlier reports [9–12, 15, 17]. Our findings may, however, suggest that the change of the mitral annulus shape (increased septolateral diameter) occurs first with continuing enlargement of the mitral annulus in all directions, signifying progression of disease.

The most important findings of our study are related to the geometry of the subvalvular apparatus and analysis of LV wall thickness. The median overall LV wall thickness was not significantly different between the groups, while some distinct areas showed thinner myocardium in patients with MR, suggesting that the area of infarction was smaller in patients with no MR. The association of the thinning of myocardial segments distal to the attachment of the PPM with the appearance of MR concurs with the recent finding from Levin's group [18]. It seems that inferior extension of an anteroapical myocardial infarction may be necessary for the development of MR. Characteristically both in our data and in the results of Levin, the muscle remained unchanged at the insertion of the PPM with only the segments distal to it being involved [18].

The other independent correlate of MR was the angle of the PPM axis against the mitral annulus plane with more leaning muscle being associated with significant regurgitation. Although we believe we are the first to describe this geometric phenomenon, it generally is in agreement with universal finding that displaced position of the PPM is the most important predictor of ischaemic MR [4, 5, 7]. Also, the increased tethering of the PPM tip (distance from contralateral annulus) harmonizes well with the literature [12, 13, 18].

The most bewildering finding of our study remains the shorter distance of the APM tip from the annulus (both ipsi- and contralateral) in the MR group. It is the only independent diastolic parameter that correlates very strongly with the presence of MR. It seems completely opposite to what is a generally accepted finding. Even though most authors agree that it is the increased PPM and not the APM tethering that is the most important in the development of ischaemic MR, the APM distance from the mitral annulus has also been described as increased [7, 11]. As we do not have serial measurements in our patients (before and after MI), we cannot say what was the APM tip to annulus distance before. However, we cannot imagine how infarction and remodelling could lead to a decreased APM tip to mitral annulus distance and how the decreased APM tethering might lead to MR. It appears to us that the most plausible explanation of our finding is that this distance represents the length of chordae tendineae, and that the development of MR is more likely in patients with originally shorter chordae. It seems logical that with short chordae, less geometric deformation in the subvalvular apparatus and mitral annulus might be needed to produce MR.

The above is obviously only a hypothesis that would require direct measurements of the chordae length. If however proved true, it might be of great clinical importance and explain some of the difficulties with the durable repair of ischaemic MR.

Limitations

The obvious limitation of our study is the resolution of CMR imaging as well as problems with unequivocal definition of some structures. A good example is the papillary muscle tip being far from a single point. We tried to overcome these obvious shortcomings by obtaining all measurements two to three times and using the median measurement for further analysis. Also, the measurements were done by the investigator blinded to the group allocation. We report the intraobserver variability.

The major lack in the analysis of the LV wall is that no late enhancement was used in the CMR imaging. Therefore, although we can discuss the geometric changes and infer about the extent of infarction based on the relative thickness of the LV wall, it is impossible to definitely state which myocardial segments are just remodelled and which are scarred.

Finally, throughout the paper, we use traditional anatomical nomenclature to describe mitral valve, its subvalvular apparatus and the left ventricle. This nomenclature has been used for years in all cardiology and cardiac surgical literature. Still, magnetic resonance images (Figs 1 and 2) clearly point to the fact that the muscle traditionally described as posteromedial is, in fact, positioned closer to the sternal surface than is its partner muscle. In reality, the papillary muscle in question, when described in attitudinally appropriate fashion, is positioned inferoseptally, with its partner located superoposteriorly. Similarly, the septal surface of the left ventricle is positioned anteriorly, with the anterior wall being really the superior one, since it is closest to the head rather than the sternum. The difference comes from the fact that traditionally the heart is described as if it was removed from the body, and positioned on its apex. Meanwhile, the magnetic resonance images display the anatomy of the heart in the context of the body.

Bearing the limitations is mind, we believe that our data confirm that the inferior extension of the anterior infarction leading to thinning of the myocardial wall distal to the PPM base, together with the change of the PPM long axis to more leaning against the long axis of the LV, are the major components resulting in the development of ischaemic MR in patients with ischaemic cardiomyopathy

due to anterior infarction. Our data also form a strong case to hypothesize that originally shorter chordae tendineae may constitute the anatomical background that makes the development of ischaemic MR with the progress of LV remodelling more likely.

SUPPLEMENTARY MATERIAL

Supplementary material is available at *EJCTS* online.

Funding

The study was performed using statutory funds of the Medical University of Silesia in Katowice, Poland.

Conflict of interest: none declared.

REFERENCES

[1] Bursi F, Enriquez-Sarano M, Nkomo VT, Jacobsen SJ, Weston SA, Meverden RA *et al*. Heart failure and death after myocardial infarction in the community: the emerging role of mitral regurgitation. Circulation 2005;111:295–301.
[2] Grigioni F, Enriquez-Sarano M, Zehr KJ, Bailey KR, Tajik AJ. Ischemic mitral regurgitation: long-term outcome and prognostic implications with quantitative Doppler assessment. Circulation 2001;103:1759–64.
[3] Lamas GA, Mitchell GF, Flaker GC, Smith SC, Gersh BJ, Basta L *et al*. Clinical significance of mitral regurgitation after acute myocardial infarction. Survival and ventricular enlargement investigators. Circulation 1997;96:827–33.
[4] Tibayan FA, Rodriguez F, Zasio MK, Bailey L, Liang D, Daughters GT *et al*. Geometric distortions of the mitral valvular-ventricular complex in chronic ischemic mitral regurgitation. Circulation 2003;108(Suppl 1):II116–21.
[5] Otsuji Y, Handschumacher MD, Liel-Cohen N, Tanabe H, Jiang L, Schwammenthal E *et al*. Mechanism of ischemic mitral regurgitation with segmental left ventricular dysfunction: three-dimensional echocardiographic studies in models of acute and chronic progressive regurgitation. J Am Coll Cardiol 2001;37:641–8.
[6] Timek TA, Lai DT, Tibayan F, Liang D, Daughters GT, Dagum P *et al*. Ischemia in three left ventricular regions: insights into the pathogenesis of acute ischemic mitral regurgitation. J Thorac Cardiovasc Surg 2003;125:559–69.
[7] Jensen H, Jensen MO, Smerup MH, Ringgaard S, Sørensen TS, Andersen NT *et al*. Three-dimensional assessment of papillary muscle displacement in a porcine model of ischemic mitral regurgitation. J Thorac Cardiovasc Surg 2010;140:1312–8.
[8] Timek TA, Lai DT, Tibayan F, Liang D, Rodriguez F, Daughters GT *et al*. Annular versus subvalvular approaches to acute ischemic mitral regurgitation. Circulation 2002;106:I27–I32.
[9] Tibayan FA, Rodriguez F, Langer F, Zasio MK, Bailey L, Liang D *et al*. Annular remodeling in chronic ischemic mitral regurgitation: ring selection implications. Ann Thorac Surg 2003;76:1549–54.
[10] Dagum P, Timek TA, Green GR, Green R, Lai D, Daughters GT *et al*. Coordinate-free analysis of mitral valve dynamics in normal and ischemic hearts. Circulation 2000;102:III62–9.
[11] Gorman JH III, Gorman RC, Jackson BM, Enomoto Y, St John-Sutton MG, Edmunds LH Jr. Annuloplasty ring selection for chronic ischemic mitral regurgitation: lessons from the ovine model. Ann Thorac Surg 2003;76:1556–63.
[12] Kaji S, Nasu M, Yamamuro A, Tanabe K, Nagai K, Tani T *et al*. Annular geometry in patients with chronic ischemic mitral regurgitation: three-dimensional magnetic resonance imaging study. Circulation 2005;112:I409–14.
[13] Kumanohoso T, Otsuji Y, Yoshifuku S, Matsukida K, Koriyama C, Kisanuki A *et al*. Mechanism of higher incidence of ischemic mitral regurgitation in patients with inferior myocardial infarction: quantitative analysis of left ventricular and mitral valve geometry in 103 patients with prior myocardial infarction. J Thorac Cardiovasc Surg 2003;125:135–43.
[14] Watanabe N, Ogasawara Y, Yamaura Y, Kawamoto T, Akasaka T, Yoshida K. Geometric deformity of the mitral annulus in patients with ischemic mitral regurgitation: a real-time three-dimensional echocardiographic study. J Heart Valve Dis 2005;14:447–52.
[15] Ahmad RM, Gillinov AM, McCarthy PM, Blackstone EH, Apperson-Hansen C, Qin JX *et al*. Annular geometry and motion in human ischemic mitral regurgitation: novel assessment with three-dimensional echocardiography and computer reconstruction. Ann Thorac Surg 2004;78:2063–8.
[16] Watanabe N, Ogasawara Y, Yamaura Y, Yamamoto K, Wada N, Kawamoto T *et al*. Geometric differences of the mitral valve tenting between anterior and inferior myocardial infarction with significant ischemic mitral regurgitation: quantitation by novel software system with transthoracic real-time three-dimensional echocardiography. J Am Soc Echocardiogr 2006;19:71–5.
[17] Hueb AC, Jatene FB, Moreira LF, Pomerantzeff PM, Kallas E, de Oliveira SA. Ventricular remodeling and mitral valve modifications in dilated cardiomyopathy: new insights from anatomic study. J Thorac Cardiovasc Surg 2002;124:1216–24.
[18] Yosefy C, Beeri R, Guerrero JL, Vaturi M, Scherrer-Crosbie M, Handschumacher MD *et al*. Mitral regurgitation after anteroapical myocardial infarction: new mechanistic insights. Circulation 2011;123:1529–36.